EINDHOVEN UNIVERSITY OF TECHNOLOGY
Department of Mathematics and Computer Science

Unsteady skin friction experimentation
in a large diameter pipe

by

A.E. Vardy, A. Bergant, S. He, C. Ariyaratne,
T. Koppel, I. Annus, A.S. Tijsseling, Q. Hou

UNSTEADY SKIN FRICTION EXPERIMENTATION
IN A LARGE DIAMETER PIPE

Alan E VARDY

University of Dundee, Scotland

Anton BERGANT

Litostroj Power d.o.o., Slovenia

Shuisheng HE, Chanchala ARIYARATNE

University of Aberdeen, Scotland

Tiit KOPPEL, Ivar ANNUS

Tallinn University of Technology, Estonia

Arris S TIJSSELING, Qingzhi HOU

Eindhoven University of Technology, The Netherlands

ABSTRACT
Experimental data for the validation of theoretical models of unsteady skin friction are limited and are available only for a few low Reynolds number flow cases. There is a strong need for detailed measurements in flows at high Reynolds numbers. In addition, there is a need for a wider range of well-controlled acceleration/deceleration rates and detailed visualization of flow structure and profiles. To address these needs, a large-scale pipeline apparatus at Deltares, Delft, The Netherlands, has been used for unsteady skin friction experiments including acceleration, deceleration and acoustic resonance tests. The apparatus consists of a constant head tank, a horizontal 200 mm diameter pipe of changeable length (44 to 49 metres) and a control valve at the downstream end. In addition to standard instrumentation, two distinctive instruments have been used: hot-film wall shear stress sensors ("direct" measurement of wall shear stress) and a PIV set-up for measurement of unsteady flow profiles. This paper describes the test rig, the instrumentation layout and the test programme. Finally, some initial test results are presented and discussed.

1. INTRODUCTION

Unsteady flows in pipes and ducts are the source of many unwanted phenomena in engineering practice. Water hammer caused by relatively sudden events such as valve closure, pump failure and water turbine emergency shut-down has been responsible for numerous pipe failures (e.g. in water, waste water, oil-hydraulic and hydro-power systems) and for unacceptable noise in workplaces. On a larger scale, pressure transients in railway tunnels are a continuing source of

discomfort to passengers on trains. Pressure transients are not *always* bad, however. They can also be used beneficially, e.g. in methods for leak detection in water supply networks and oil pipelines, and in the good old hydraulic ram.

Friction and consequential damping in unsteady flows can significantly reduce the harmful effects of some pressure transients and can have a strong influence on behaviour close to resonance. It is well known that *the classical approach* [1], [2] suffers from a lack of damping of pressure waves, leading to conservative results. Unsteady skin friction distorts the *shapes* of wave fronts. As a consequence, phase shifts are introduced in measurements of pressure amplitudes. Unsteady skin friction is crucial in the evolution of pressure wavefronts propagating along railway tunnels. It has a decisive influence on the wavefront steepening process that determines whether unacceptable sonic booms will occur. It is clear that the magnitude of unsteady friction in one-dimesional (1-D) bulk flow depends on the system under analysis.

Unsteady friction arises from extra losses associated with the 2-D (and sometimes 3-D) nature of unsteady velocity profiles. If turbulence is considered, unsteady friction is always a 3-D problem; however, modelling either 2-D or 3-D cases is computationally intensive [3]. It is desirable to have a model that takes into account higher dimensional velocity profile behaviour, but that can be implemented efficiently in 1-D models. A number of unsteady friction models have been reviewed in the literature [4], [5]. In engineering practice, two distinct models are used for the simulation of unsteady friction in 1-D analyses of unsteady flow, i.e. the Brunone *et al.* model [6] and the Zielke model [7]. The simpler Brunone *et al.* model assumes that the amplitude of the phenomenon scales with the instantaneous acceleration of the liquid. However, the range of applicability of this model, and the values of some necessary empirical coefficients, need to be more clearly established [8]. The more complex Zielke model (quasi-2-D weighting function model) is based on instantaneous and weighted past velocity profiles (history effects). Weighting functions have been developed theoretically for transient laminar flow [7] and for transient turbulent flow [9], [10]. This approach offers potential for use without the need for (new) empirical data. The above models cannot yet be considered complete. For the 1-D model, it is not yet known how to make reliable estimates of the necessary empirical coefficients. For the quasi-2-D model, the key unknown is the underlying *frozen-viscosity* distribution that is, at best, only approximately valid and, even then, only for short times. In some simple flows (e.g. uniform acceleration), neither method predicts the *sign* of the unsteady component of friction reliably, let alone its amplitude. To address this, we need a better understanding of the actual behaviour of unsteady friction in different types of flow.

Developers and users of unsteady skin friction models need full-scale data with which to compare their models. Unfortunately, experimental data for validation are limited and are available only for a few low Reynolds number flow cases. There is a strong need for detailed measurements in flows at higher Reynolds numbers. In addition, there is a need for a wider range of well-controlled acceleration/deceleration rates and detailed visualization of flow structure and profiles. To address these needs, a large-scale pipeline apparatus at Deltares, Delft, The Netherlands, has been used for unsteady skin friction experiments including acceleration, deceleration and acoustic resonance tests. The apparatus consists of a constant head tank at the upstream end (head of 25 metres), a horizontal 200 mm diameter pipe of changeable length (44 to 49 metres) and a control valve at the downstream end. A globe type control valve connected to a high head tank has been used for acceleration and deceleration tests. A frequency-controlled rotating valve discharging into the open atmosphere has been used for resonance tests. In addition to standard instrumentation, two distinctive instruments have been used: hot-film wall shear stress sensors ("direct" measurement of wall shear stress)

and a PIV set-up for the measurement of unsteady flow profiles. This paper describes the test rig, the instrumentation and the test programme. Finally, some initial test results are presented and discussed.

2. TEST RIG AND INSTRUMENTATION LAYOUTS

A large-scale pipeline apparatus, where large scale implies large Reynolds numbers (up to 400,000), has been used for the unsteady skin friction experiments. The horizontal steel pipeline has an internal diameter of 206 mm, changeable length (44 m to 49 metres) and is supplied from a 25 m head reservoir at its upstream end (see Figs.1 and 2).
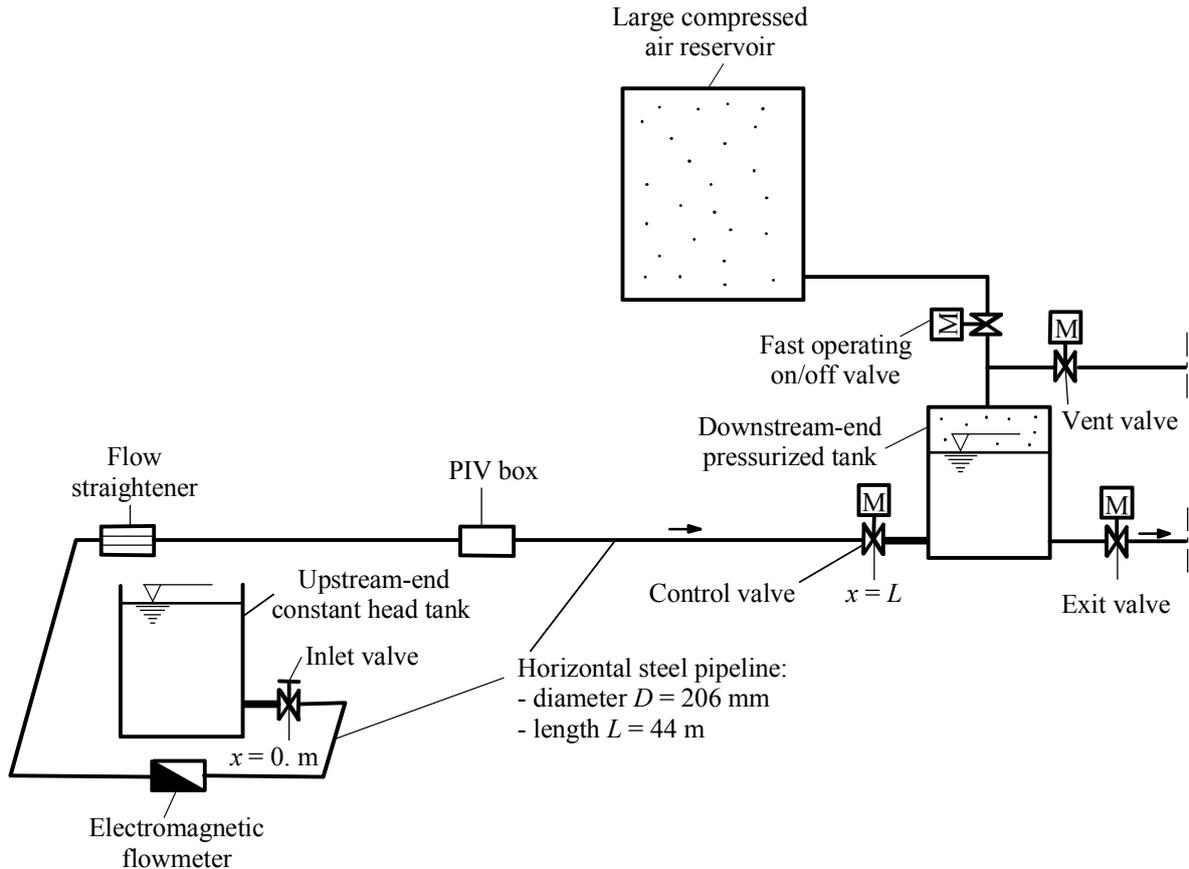

Fig.1 Test rig for accelerating & decelerating flows

Three types of transient turbulent flow have been investigated in the apparatus:

(1) non-reversing accelerating & decelerating flow
(2) reversing accelerating & decelerating flow
(3) oscillatory (pulsating) flow (including resonance & water hammer tests)

For non-reversing and reversing acceleration & deceleration flows, the pipe has a length of 44 m - see Fig.1. The downstream-end high-head tank is vented for non-reversing flow tests (atmospheric pressure). Acceleration from zero flow and ramp-up & ramp-down flows are controlled by a downstream-end globe type valve (initially by a butterfly type valve). The reversing accelerating & decelerating flows are controlled by the pressurized downstream-end tank instead of by the globe valve. Transient events are induced by opening of a fast operating

on/off valve (Fig.1). The pressure gradient accelerates an initially zero flow or decelerates (and possibly reverses) an initially steady state flow.
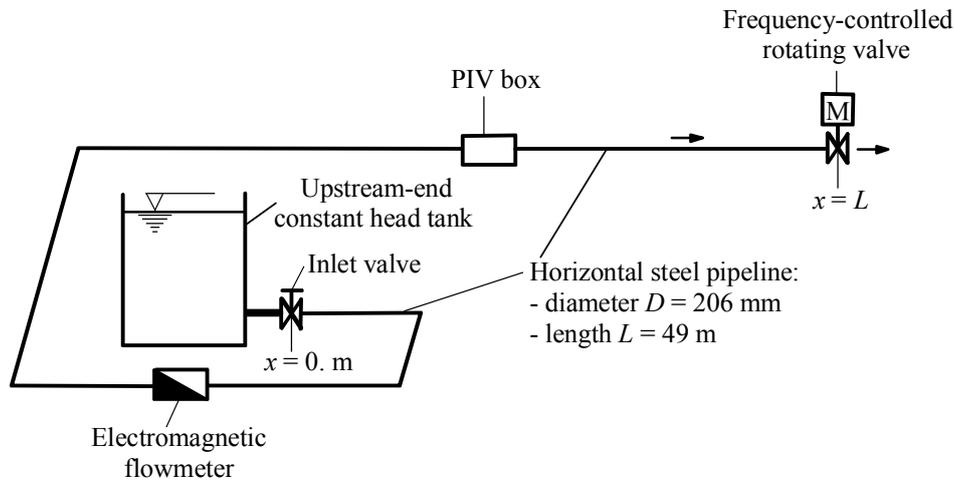

Fig.2 Test rig for oscillatory (pulsating) flow

The apparatus has been modified for oscillatory (pulsating) flow tests. The pipe has a length of 49 m - see Fig.2. The key element is a rotating valve that generates harmonically oscillating flow rates and pressures. A Svingen type frequency-controlled rotating valve is used in the apparatus [11]. The valve consists of an end-flange with a sluice gate and a teflon disc driven by a frequency-controlled electromotor (5 kW). The frequency of oscillation can be varied between 3 and 100 Hz. At a constant head upstream-end tank, the flow rate amplitude is adjusted by the opening of the sluice gate (maximum opening 800 mm^2) and the amplitude of the disc (10 mm in our tests). In addition, water hammer tests can be performed in this oscillatory flow apparatus. A 25 mm diameter ball is installed at the end-flange of the oscillating valve. In this case, the sluice gate is closed and the water hammer event is initiated by rapid closure of the ball valve (for the oscillating flow tests, the ball valve is closed).

2.1 Instrumentation

The instruments used for unsteady skin friction measurements have been carefully selected (accuracy, frequency response) and calibrated prior to and after the dynamic measurements. The sampling frequency for each continuously measured quantity (except PIV) was $f_s = 1,000$ Hz. For high Reynolds number cases, the high-speed PIV camera was set to record at a frequency of $f_s = 3,000$ Hz, whereas for lower Reynolds number cases, it was $f_s = 2,000$ Hz and $f_s = 1,000$ Hz.

The layout of dynamic instruments in the test section for non-reversing and reversing acceleration & deceleration flows is depicted in Fig.3. The following quantities have been measured continuously (pipe length $L = 44$ m):
- valve position
- pressure (close to the downstream end valve (app. 1/10 of the pipe length from the control valve), close to the PIV box (app. 1/4 of the pipe length from the control valve) and app. 2/5 of the pipe length from the control valve)
- velocity profile (PIV box)
- wall shear stress (6 sensors; 3 at the PIV box and 3 app. 1 m upstream of the PIV box)
- differential pressure (length between the taps is app. 3/10 of the pipe length)

4

- water temperature
- flow rate (2 electromagnetic flowmeters at 2/3 of pipe length from the control valve)
- flow direction (reversing flow tests only)
- differential pressure between the downstream-end pressurized tank and the pipe (reversing flow tests only)
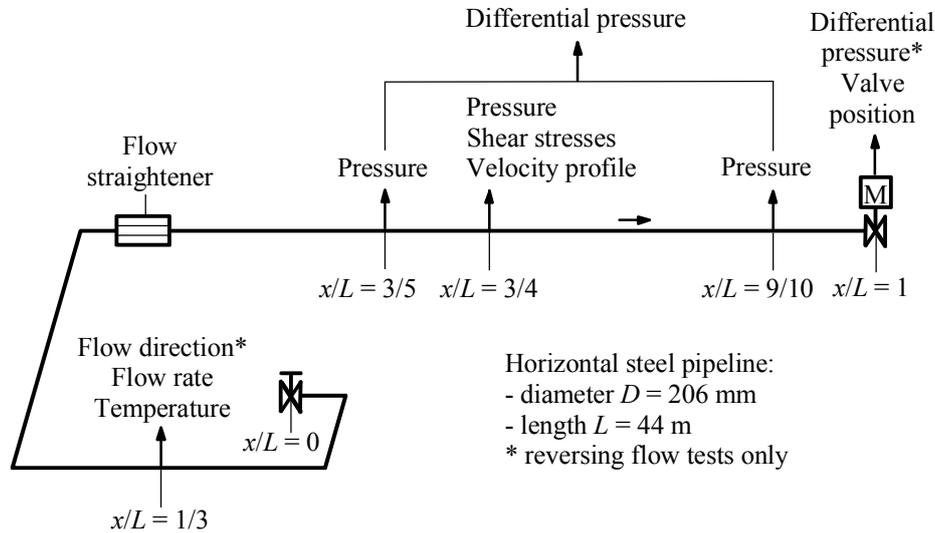

Fig.3 Layout of dynamic instruments in test section for non-reversing and reversing acceleration & deceleration flows

Pressures were measured by strain-gauge pressure transducers. PIV measurements were carried out using a high-speed camera and a powerful laser for lighting. The camera was adjusted so that it covered nearly the pipe radius (from the top of the pipe to the centre). The size of a window used was 512×1024 pixels. For high Reynolds number cases, the laser was set to the maximum power. For lower Reynolds number cases, the power was decreased. Hydrogen bubbles were used for seeding. They were produced by an electrified rod inserted in the flow at the upstream side as close as possible to the Perspex box. One PC was dedicated to the PIV measurements using special software DaVis 8.0. The wall shear stress τ_w was measured at three equidistant circumferential positions at two axial locations along the pipeline. The discharge was measured by a fast response electromagnetic flowmeter.

The layout of the dynamic instruments in the test section for oscillatory (pulsating) flow is depicted in Fig.4. The following quantities have been measured continuously (pipe length L = 49 m):
- pressure at the valve
- pressure at PIV box (4/13 of pipe length from the rotating valve)
- pressure at electromagnetic flowmeter (3/5 of pipe length from the rotating valve)
- pressure at the upstream end
- velocity profile (PIV box)
- wall shear stress (6 sensors; 3 at the PIV box and 3 app. 1 m upstream of the PIV box)
- differential pressure
- water temperature
- flow rate (electromagnetic flowmeter at 3/5 of pipe length from the rotating valve)
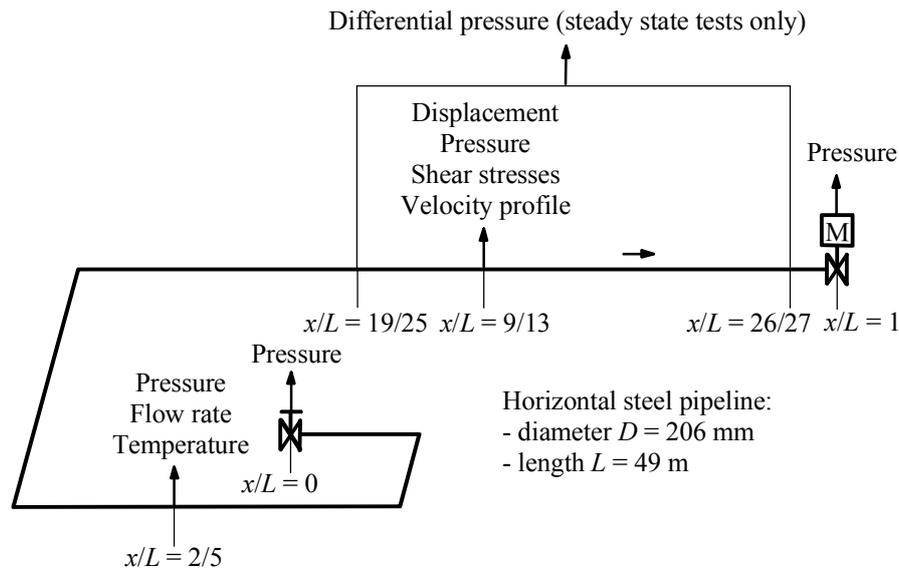- pipe vibrations (displacement transducer close to the PIV box)

Fig.4 Layout of dynamic instruments in test section for oscillatory (pulsating) flow

Pressures were measured by piezoelectric pressure transducers and pipe displacements were measured by a laser-Doppler displacement transducer.

3. TEST PROGRAMME

A comprehensive test programme on unsteady skin friction in a large-scale pipeline apparatus (Figs.1 and 2) was carried out in 2008. Three types of experimental runs were performed including acceleration, deceleration and acoustic resonance (oscillatory flow) tests.

In the first test period the non-reversing accelerating & decelerating flow tests were performed in the rig for decelerating & accelerating flows (Fig.1). These include:
(1) Acceleration from zero flow: **Re** from 0 to 400,000 (**Re** = Reynolds number: $\mathbf{Re} = VD/v$,
   V = instantaneous average flow velocity, D = pipe diameter, v = kinematic viscosity)
(2) Acceleration from an initially steady turbulent flow:
   Re from {10,000 to 30,000} to {120,000 to 220,000}
(3) Deceleration from an initially steady turbulent flow:
   Re from {25,000 to 60,000} to {3,000 to 15,000}
The non-reversing type flows were controlled by the downstream-end globe type valve.

Next two types of reversing accelerating & decelerating flow tests were carried out in the test rig shown in Fig.1:
(1) Acceleration from zero flow: pressure difference between the downstream-end pressurized tank and the pipe Δp from 5 to 420 kPa
(2) Deceleration from an initially steady turbulent flow: **Re** from {50,000 and 300,000};
   pressure difference between the downstream-end pressurized tank and the pipe Δp from 5 to 420 kPa
These flows were controlled by the pressure difference between the downstream-end pressurized tank and the pipeline.

Oscillatory (pulsating) flow tests including water hammer tests have been performed in the test rig shown in Fig.2. These include:
(1) Quasi-steady tests (slowly rotating the valve by hand): $\mathbf{Re}_{ave}$ = 22,000

6

($\mathbf{Re}_{ave} = V_{ave}D/\nu$, V_{ave} = average flow velocity per cycle)
(2) Oscillatory flow tests (oscillating valve): $\mathbf{Re}_{ave} = 22{,}000$
    (The frequency of oscillation varied between 3 and 100 Hz.)
(3) Water hammer tests (rapid closure of 1 inch valve): $\mathbf{Re}_0 = 25{,}000$
    ($\mathbf{Re}_0 = V_0D/\nu$, V_0 = initial (steady-state) average flow velocity)
In quasi-steady and oscillatory flow tests the opening of the sluice gate varied between
80 mm^2 (minimum) and 240 mm^2 (maximum). The sluice gate was closed for water hammer
tests. Water hammer events were initiated by rapid manual closure of the ball valve that was
mounted at the end-flange of the rotating (oscillating) valve.

4. UNSTEADY FRICTION TESTS

This section presents initial results of measurements that have been processed and analysed.
The case study deals with uniformly accelerating flow from initial $\mathbf{Re}_0 = 11{,}700$ to final $\mathbf{Re}_f = 114{,}400$. The acceleration was achieved using a downstream-end globe control valve (Fig.1).
The time period for flow ramp-up was $T_{up} = 10.75$ s. Measurements of two key quantities, the
wall shear stress τ_w and the axial flow velocity profile $V(y,t)$ (y = distance in radial direction;
at pipe wall: $y = 0$ mm), are presented and discussed.

4.1 Wall Shear Stress Results

Shear stress (hotfilm) sensors were calibrated using pressure measured for a series of steady
flows by a differential pressure transducer. The calibration was checked with that of flow
measurement using the Haaland equation [12]. The results shown are ensemble-averaged
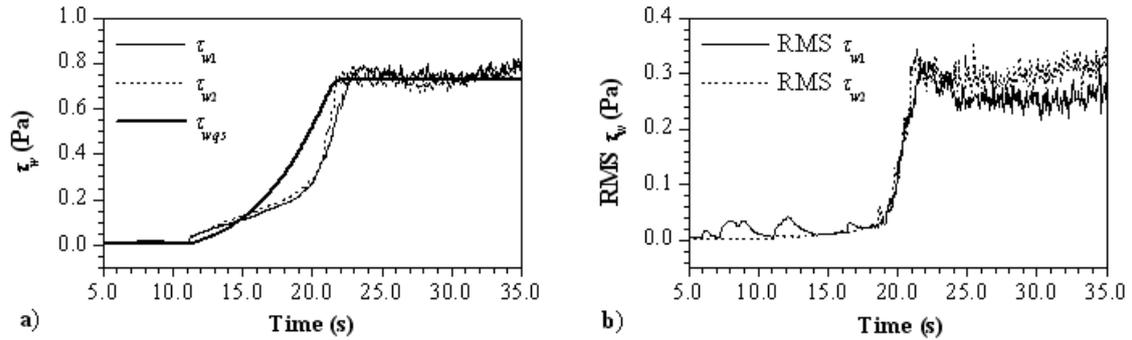values of 125 careful repetitions of the flow excursion.

Fig.5 Ensemble-averaged wall shear stress (τ_w) and RMS variation of wall shear stress (RMS τ_w) for ramp-up flow case ($\mathbf{Re}_0 = 11{,}700$; $\mathbf{Re}_f = 114{,}400$; $T_{up} = 10.75$ s): 1 – at PIV box; 2 – 1 m upstream of the PIV box; qs – quasi-steady.

Examination of shear stresses at the PIV box (τ_{w1}) and 1 m upstream of the box (τ_{w2}) (both
stresses are measured at the same circumferential position) reveals that the wall shear stress in
the unsteady flow initially over-responds to the acceleration compared to the quasi-steady
stress (τ_{wqs}). This effect can be seen at time of about 11 seconds - see Fig.5(a). It should be
noted that the quasi-steady curve is based on measurements in steady flow for over ten
different flow rates. Thereafter, the increase in the wall shear stress reduces and it eventually
becomes less than the quasi-steady value. Later, there is a second rapid rise in the wall shear
stress and it approaches the quasi-steady values again. This variation was analysed and
discussed in a paper by He *et al.* [5] with the use of RANS CFD data, and it is the result of the
opposing effects of inertia and delays in turbulence response. Fig.5(b) provides further

evidence of the frozen turbulence response predicted in [5]: RMS of τ_w shows little response up to a time of about 19 seconds; then it increases rapidly as turbulence starts to respond. The sudden increase in the wall shear stress is observed shortly after this.

4.2 Particle Image Velocimetry Results

Particle image velocimetry (PIV) was carried out on 29 of the repeats for the case considered. Due to the large scale of the apparatus it was necessary to use localized seeding (hydrogen bubbles). The PIV data have been carefully processed and filtered to reduce noise and erroneous flow vectors. In Fig.6 'tt' indicates time-steps as time progresses ($\Delta tt = 20$ corresponds to 0.4 s). The value of y in Fig.6 indicates the distance from the wall as a proportion of the pipe area that was photographed. At tt = 40, the flow is steady (**Re** = 11,700) - just before the onset of acceleration.
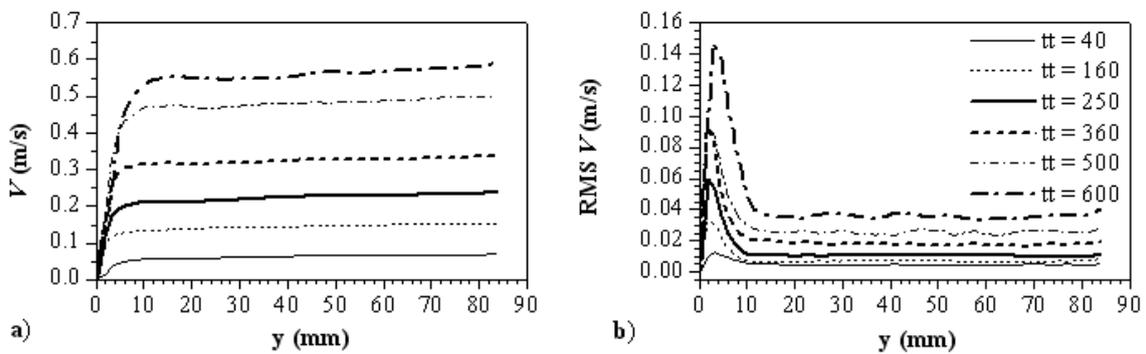

*Fig.6 Ensemble-averaged velocity profile (**V**) and RMS of velocity (RMS **V**) for ramp-up flow case ($\textbf{Re}_0$ = 11,700; $\textbf{Re}_f$ = 114,400; T_{up} = 10.75 s): Δtt = 20 corresponds to 0.4 s.*

Fig.6(a) illustrates the velocity profile obtained from PIV at different instances during the acceleration. The *shape* of the velocity profile in the core remains practically unchanged for a long duration of time. On the other hand, near-wall velocity increases with high velocity gradients evolving immediately. The RMS variation of velocity in Fig.6(b) shows that there is a slow increase in the core region of the flow. Near the wall, at $y \approx 1$ mm, there is a rapid increase which appears to propagate outwards as time progresses in Fig.6(b). The bulk flow acceleration causes the velocity in the core to increase at a constant rate. However, near the wall the no-slip condition at the wall causes large velocity gradients. With time, the influence of the wall constraint slowly propagates towards the pipe core. Turbulence first responds in an annular near-wall region and this production response propagates away from the wall as the velocity profile responds to the no-slip condition [5]. The imposed acceleration in this particular case is relatively high and therefore little response is observed in turbulence away from the wall region. The turbulence production and propagation delays are large here.

5. CONCLUSIONS

Developers and users of unsteady skin friction models need full-scale data with which to compare their models. Unfortunately, experimental data for validation are limited and are available only for a few low Reynolds number flow cases. This research focuses on detailed measurements in flows at higher Reynolds numbers. A large-scale pipeline apparatus at Deltares, Delft, The Netherlands, has been used for unsteady skin friction experiments including acceleration, deceleration and acoustic resonance tests. Two distinctive instruments have been used: hot-film wall shear stress sensors ("direct" measurement of wall shear stress)

and a PIV set-up for measurement of unsteady flow profiles. The case study dealing with uniformly accelerating flow clearly shows the effect of unsteadiness on wall shear stresses and velocity profiles, which are significantly different from the classical quasi-steady flow results.

6. ACKNOWLEDGEMENTS

7. REFERENCES

[1]   Wylie, E.B., Streeter, V.L.: *Fluid Transients in Systems.* Prentice Hall. Englewood Cliffs. 1993.

[2]   Bergant, A., Tijsseling, A.S., Vítkovský, J.P., Covas, D.I.C., Simpson, A.R., Lambert, M.F.: Parameters Affecting Water-Hammer Wave Attenuation, Shape and Timing-Part 1: Mathematical Tools & Part 2: Case Studies. *Journal of Hydraulic Research. IAHR.* **46**. 2008. pp. 373-381 & 382-391.

[3]   Abreu, J., de Almeida, A.B.: Timescale Behaviour of the Wall Shear Stress in Unsteady Laminar Pipe Flows. *Journal of Hydraulic Engineering. ASCE.* **135**. 2009. pp. 415-424.

[4]   Bergant, A., Simpson, A.R., Vítkovský, J.P.: Developments in Unsteady Flow Friction Modelling. *Journal of Hydraulic Research. IAHR*. **39**. 2001. pp. 249-257.

[5]   He, S., Ariyaratne, C., Vardy, A.E.: A Computational Study of Wall Friction and Turbulence Dynamics in Accelerating Pipe Flows. *Computers & Fluids*. **37**. 2008. pp. 674-689.

[6]   Brunone, B., Golia, U.M., Greco, M.: Modelling of Fast Transients by Numerical Methods. *International Meeting on Hydraulic Transients with Column Separation. 9th Round Table. IAHR.* 1999. pp. 215-222.

[7]   Zielke, W.: Frequency-Dependent Friction in Transient Pipe Flow. *Journal of Basic Engineering. ASME.* **90**. 1968. pp. 109-115.

[8]   Bughazem, M.B., Anderson, A.: Investigation of an Unsteady Friction Model for Waterhammer and Column Separation. *Pressure Surges. Safe Design and Operation of Industrial Pipe Systems. BHR Group.* 2000. pp. 483-498.

[9]   Vardy, A.E., Brown, J.M.B.: Transient Turbulent Friction in Smooth Pipe Flows. *Journal of Sound and Vibration.* **259**. 2003. pp. 1011-1036.

[10] Vardy, A.E., Brown, J.M.B.: Transient Turbulent Friction in Fully-Rough Pipe Flows. *Journal of Sound and Vibration*. **270**. 2004. pp. 233-257.

[11] Svingen, B.: *Fluid Structure Interaction in Piping Systems*. PhD thesis. NTNU Trondheim. 1996.

[12] Haaland, S.E.: Simple and Explicit Formulas for the Friction Factor in Turbulent Pipe Flow. *Journal of Fluids Engineering. ASME*. **105**. 1983. pp. 89-90.

8. NOMENCLATURE

D	(m)	pipe diameter	V	(m.s^{-1})	average flow velocity
f_s	(Hz)	sampling frequency	x	(m)	axial distance
L	(m)	length	y	(m)	radial distance
Re	(-)	Reynolds number	Δp	(Pa)	pressure difference
T_{up}	(s)	ramp-up time	Δtt	(-)	'tt' interval
t	(s)	time	ν	(m^2.s^{-1})	kinematic viscosity
tt	(-)	number of time steps	τ_w	(Pa)	wall shear stress
V	(m.s^{-1})	flow velocity			

Subscripts:

ave	average per cycle	0	initial conditions
f	final	1	at PIV box
qs	quasi-steady	2	1 m up. of PIV box

Abbreviations:

PIV	particle image veloc.	RMS	root mean square

9. APPENDIX: Errors in Vardy & Brown, *J Hyd Engrg, ASCE* (2007): 133(11), 1219-1228

The authors wish to draw attention to two errors and an omission in a recent paper by Vardy & Brown on unsteady skin friction. The errors are not fundamental to the main purpose of the paper, but they have the potential to cause unnecessary wasted time for researchers using the results of the paper in detail.

Error-1: The coefficients listed after Eq.17 on page 1226 are incorrect. Correct values are given in *J Hyd Engrg*, ASCE (2009): **135**(1), 71.

Error-2: The graphs presented in Fig 2a are labelled **Re** = 10^8, 10^7, 10^6, 10^5, 10^4, 10^3. Unfortunately, the data used to draw these graphs were taken from the wrong columns of a spreadsheet. The graphs shown in the figure are actually for **Re** = $10^{7.5}$, $10^{6.5}$, $10^{5.5}$, $10^{4.5}$, $10^{3.5}$, $10^{2.5}$. This error applies to Fig 2a only. The graphs shown in Fig 2b are labelled correctly.

Omission: Graphical results are presented for a very large range of roughnesses – up to $k_s/D = 0.1$ – and for a large range of Reynolds numbers - up to **Re** = 10^8. In addition, interpolation formulae are presented to enable the data to be used in computer software. However, the limits of validity of the interpolation formulae are not detailed. The authors consider the formulae to be sufficient for practical purposes over the whole range presented. Note, however, that the accuracy of the B^{**} formulae reduces slightly at very small and very large values of k_s/D, especially at very large Reynolds numbers.

PREVIOUS PUBLICATIONS IN THIS SERIES:

Number	Author(s)	Title	Month
09-37	E.J.W. ter Maten T.S. Doorn J.A. Croon A. Bargagli A. Di Bucchianico O. Wittich	Importance sampling for high speed statistical Monte-Carlo simulations	Nov. '09
09-38	J. Rommes P. Lenaers W.H.A. Schilders	Reduction of large resistor networks	Nov. '09
09-39	T.S. Doorn J.A. Croon E.J.W. ter Maten A. Di Bucchianico	A yield centric statistical design method for optimization of the SRAM active column	Dec. '09
09-40	C.G. Giannopapa J.M.B. Kroot A.S. Tijsseling M.C.M. Rutten F.N. van de Vosse	Wave propagation in thin-walled aortic analogues	Dec. '09
09-41	A.E. Vardy A. Bergant S. He C. Ariyaratne T. Koppel I. Annus A.S. Tijsseling Q. Hou	Unsteady skin friction experimentation in a large diameter pipe	Dec. '09